

## FACTORS INFLUENCING THE IDEALITY FACTOR OF SEMICONDUCTOR p-n AND p-i-n JUNCTION STRUCTURES AT CRYOGENIC TEMPERATURES

 Jo'shqin Sh. Abdullayev<sup>a\*</sup>,  Ibrokhim B. Sapaev<sup>a,b</sup>

<sup>a</sup>National Research University TIIAME, Department of Physics and Chemistry, Tashkent, Uzbekistan

<sup>b</sup>Western Caspian University, Baku, Azerbaijan

\*Corresponding Author e-mail: [j.sh.abdullayev6@gmail.com](mailto:j.sh.abdullayev6@gmail.com)

Received July 9, 2024; revised October 9, 2024 accepted October 18, 2024

This article elucidates the dependence of the ideality factor on both internal functional parameters and external factors in semiconductors at low temperatures. We have explored the influence of external factors such as temperature and external source voltage. Through numerical modeling and theoretical analysis, we thoroughly investigate the dependencies of semiconductor material internal functional parameters—including doping concentration, the bandgap of semiconductors, the lifetime of charge carriers, and geometric dimensions ranging from micrometers to nanometers—the ideality factor on p-n and p-i-n junction structures. Our analysis spans cryogenic temperatures from 50 K to 300 K, with intervals of 50 K. To conduct this study, we have focused on p-n and p-i-n junction structures fabricated from Si and GaAs. The selected model features geometric dimensions of  $a=10\ \mu\text{m}$ ,  $b=8\ \mu\text{m}$ , and  $c=6\ \mu\text{m}$ . The thickness of the i-layer ranged from  $10\ \mu\text{m}$  to  $100\ \mu\text{m}$  in  $10\ \mu\text{m}$  increments. Increasing the thickness of the i-layer results in a corresponding rise in the ideality factor.

**Keywords:** *p-n junction; p-i-n junction; SRH recombination; Internal functional parameters; External factors; Ideality factor; Cryogenic temperatures*

**PACS:** 73.40.Lq, 73.61.Cw, 73.61.Ey, 72.20.Jv

### INTRODUCTION

This factor evaluates the ideality of p-n and p-i-n junction structures and assists in assessing the current mechanisms through numerical and theoretical modeling. The attributes and functionality of p-i-n and p-n junction diodes are intimately connected to the conduct of carriers at the interface established between p-type and n-type materials. These junctions serve as the fundamental building blocks for many other electronic devices, and the analytical techniques applied to understand p-i-n and p-n junctions can be extended to solve various electronic problems. The kinetic processes of electrons and holes at p-n and p-i-n junctions are explained through two mechanisms: drift-diffusion and recombination-generation. The ideality factor serves as a distinguishing parameter between these mechanisms, theoretically falling within the range of 1 to 2 [1]. However, several experiments have shown that the ideality factor often exceeds 2 [2-3]. The primary objective of this work is to discuss the relationship between forward voltage, temperature, the thickness of the i-layer, and material parameters, all of which are dependent on the ideality factor. Numerous scientific articles have explored the correlation between the ideality factor and temperature [4-8], although these studies have typically not covered a broad temperature range. Characteristics of thermosensors at cryogenic temperature were studied [9].

While numerous articles [10-12] have investigated the ideality factor, its true nature and the parameters influencing it remain incompletely understood. Variations in ideality factor values across different materials [13] underscore the importance of comprehensively studying the dependence of materials on their functional parameters. To address this gap, this work focuses on studying the ideality factor of p-n and p-i-n junction structures fabricated from Si and GaAs materials. Overall, operating semiconductor devices at cryogenic temperatures is essential for a wide range of scientific and technological applications, enabling advancements in fields such as quantum computing, astrophysics, materials science, and high-energy physics. At cryogenic temperatures, semiconductor devices often exhibit improved electrical characteristics, such as reduced noise, increased carrier mobility, and lower leakage currents. This can lead to enhanced device performance, including higher-speed operation, improved signal-to-noise ratios, and lower power consumption.

Some semiconductor materials, such as certain types of doped silicon and germanium, exhibit superconducting behavior at cryogenic temperatures. Cryogenic temperatures are essential for the operation of many quantum computing architectures, which often rely on semiconductor-based qubits. In astrophysics and space exploration, semiconductor devices operating at cryogenic temperatures are used in instruments such as infrared detectors, spectrographs, and low-noise amplifiers. Cryogenic temperatures are often employed in materials research to investigate the electronic properties of semiconductors, including bandgap engineering, electron mobility, and quantum confinement effects. In experiments conducted at particle accelerators and high-energy physics laboratories, semiconductor detectors cooled to cryogenic temperatures are used to measure the energy and trajectories of charged particles produced in collisions.

### MATERIALS AND METHODS

In the ideal scenario, the relationship between the current density and the voltage passing through the p-n and p-i-n junction structures is expressed as follows.

**Cite as:** J.Sh. Abdullayev, I.B. Sapaev, East Eur. J. Phys. 4, 329 (2024), <https://doi.org/10.26565/2312-4334-2024-4-37>

© J.Sh. Abdullayev, I.B. Sapaev, 2024; CC BY 4.0 license

$$J = J_S \left( \exp\left(\frac{qU_{p-n}}{mkT}\right) - 1 \right), \tag{1}$$

where  $U_{p-n}$  is p-n junction voltage,  $q$  is the elementary electron charge,  $J_S$  is referred to as the saturation current density in the reverse connection, and its value is determined as follows:

$$J_{S1} = qn_i^2 \left( \frac{D_p}{L_p N_D} + \frac{D_n}{L_n N_A} \right). \tag{2a}$$

Where  $n_i$  intrinsic concentration,  $D_{p,n}$  and  $L_{p,n}$  are diffusion coefficient and length of electrons and holes respectively.  $N_D$  and  $N_A$  are donors and acceptors. The diffusion length  $L_D$  for silicon with resistivity values of 10  $\Omega$ cm and 100  $\Omega$ cm, and carrier lifetimes of 8 $\mu$ s and 3 $\mu$ s for electrons and holes, respectively, is approximately  $L_{p,n} \approx 100 \mu\text{m}$ . If the current transport mechanism relies on a drift-diffusion mechanism, then expression (2a) is appropriate. Conversely, if the current transport mechanism is driven by a recombination-generation mechanism, it is determined from expression (2b).

$$J_{S2} = \frac{qn_i \cdot d_{p-n}}{2\tau_{eff}} \tag{2b}$$

Another crucial aspect of the ideality factor  $m$  is its role in determining the recombination mechanism in the p-n junction. Experiment and theoretical calculations indicate that the ideality factor is inversely proportional to temperature as follows expression.

$$m(T) = \frac{q}{kT} \cdot \frac{U_{p-n}}{\ln\left(\frac{I(T,U)}{I_S(T)} + 1\right)} \tag{3}$$

We express the ideality factor using expression (4). Through theoretical calculations, we aimed to determine the parameters on which  $A(T)$  and  $C(T)$  coefficients depend. The coefficients  $A(T)$  and  $C(T)$  are assumed to represent both the internal functional parameters and external factors of the semiconductor material.

$$m(T) = A(T) + \frac{C(T)}{T} \tag{4}$$

The expression (4) was employed to analytically ascertain the temperature dependence of the ideality factor for p-n junctions based on Si and GaAs, covering temperatures from 50 K to 300 K with intervals of 50 K. The band gap of the semiconductor depends on the size [14].

The thickness of the i-layer ranged from 10  $\mu\text{m}$  to 100  $\mu\text{m}$  in 10- $\mu\text{m}$  increments. Increasing the thickness of the i-layer results in a corresponding rise in the ideality factor. The thesis chose Si semiconductor materials, incorporating boron doping at a concentration of 3e17  $\text{cm}^{-3}$  to create the pSi-layer and phosphorus doping at a concentration of 4e18  $\text{cm}^{-3}$  for the nSi-layer. The diffusion length  $L_D$  for silicon with resistivity values of 10  $\Omega$ cm and 100  $\Omega$ cm, and carrier lifetimes of 8 $\mu$ s and 3 $\mu$ s for electrons and holes, respectively, is approximately  $L_D \approx 100 \mu\text{m}$ .

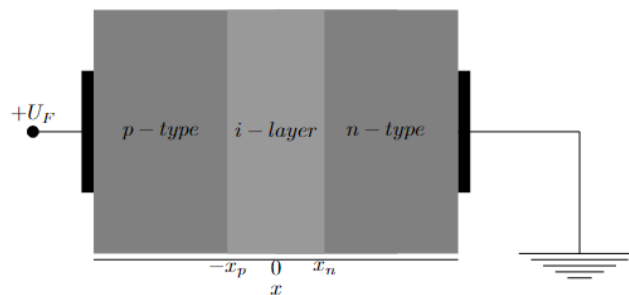


**Figure 1.** The schematic depicting a 2D cross-section of our model planar p-i-n junction,  $U_F$  is forward voltage. The light grey area represents the i-layer region, while the dark grey areas represent the quasi-neutral (QNR) fields in the p-type and n-type regions, respectively

The selected model features geometric dimensions of  $a=10 \mu\text{m}$ ,  $b=8 \mu\text{m}$ , and  $c=6 \mu\text{m}$ . Within the electrophysical models, certain distinctions are noted: the gap width fluctuates with temperature [15], while the mobility of electrons and holes is influenced by both temperature and concentration [16]. Moreover, variations in Shockley-Read-Hall (SRH) recombination are observed in response to changes in temperature and doping concentration [17]. Recombination in p-n and p-i-n junctions at low temperatures shows distinct characteristics compared to room temperature behavior due to changes in carrier dynamics and material properties. Recombination Mechanisms are mainly three types. Radiative

Recombination, Non-Radiative Recombination, Surface Recombination. The results obtained from the models and samples employed in this section are thoroughly presented and scrutinized in Section RESULTS AND DISCUSSION.

**RESULTS AND DISCUSSION**

In this section, the results are presented and analyzed. The various current lines observed in Figure 2 at low voltage can be explained as follows. The results are depicted in Figure 2, showcasing both semi-logarithmic (a) and linear (b) I-U characteristics. It is evident from the figures that there is a decrease in current as the layer thickness increases.

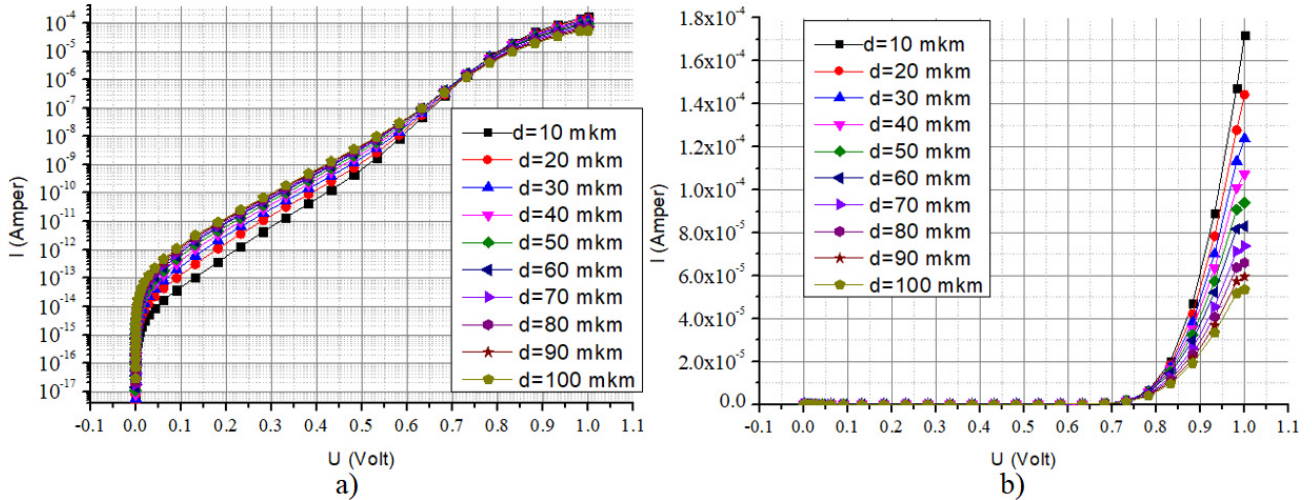


**Figure 2.** Volt-Amper characteristic of p-i-n junction based on Si a) Semi-logarithmic, b) linear, d is the thickness *i*-layer

Figure 3 (b) illustrates the dependency of the ideality factor (*i*) on the layer thickness at 0.2, 0.4, 0.6, and 0.8 volts.

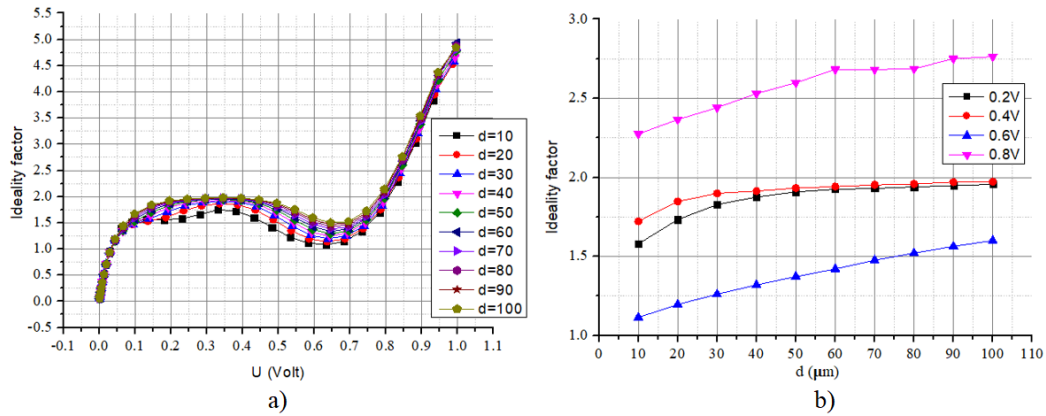


**Figure 3.** Ideality factor of the p-i-n junction dependent on a) forward voltage, b) the thickness of the *i*-layer

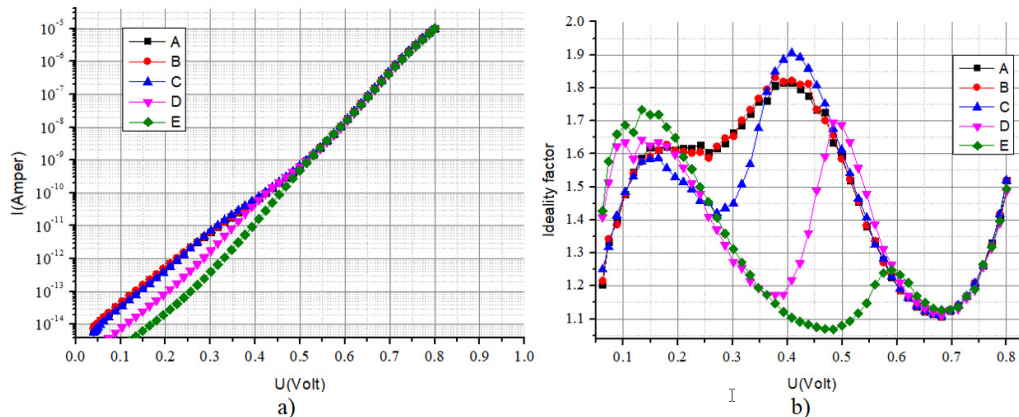


**Fig. 4.** a) The semi-logarithmic volt-ampere characteristic of a p-i-n junction, b) the ideality factor of the p-i-n junction as a function of forward voltage, across different intrinsic doping concentrations of the *i*-layer

The I-U characteristic of the p-i-n junction structure made of Si material is provided, wherein the intrinsic field concentration was studied for cases A, B, C, D, and E. The intrinsic concentration of silicon is typically  $n_i \approx 10^{10} \text{ cm}^{-3}$ , however, in this scenario,  $n_i = 10^{11} \text{ cm}^{-3}$  for case A,  $n_i = 10^{12} \text{ cm}^{-3}$  for case B,  $n_i = 10^{13} \text{ cm}^{-3}$  for case C,  $n_i = 10^{14} \text{ cm}^{-3}$  for case D, and  $n_i = 10^{15} \text{ cm}^{-3}$  for case E were observed. From Figure 4, we can see that in the range from 0 volts to 0.5 volts, there are different lines of current strength at different values of doping concentration, and at values greater than 0.5 volts, they almost all overlap. This situation can be explained as follows: recombination processes were observed between 0 and 0.5 volts, while the drift-diffusion mechanism prevailed above 0.5 volts. Recombination processes with different values were observed for different concentration levels. In the case of E, where  $n_i = 10^{15} \text{ cm}^{-3}$ , it is shown that the drift-diffusion current prevails even at low voltages and high concentration values.

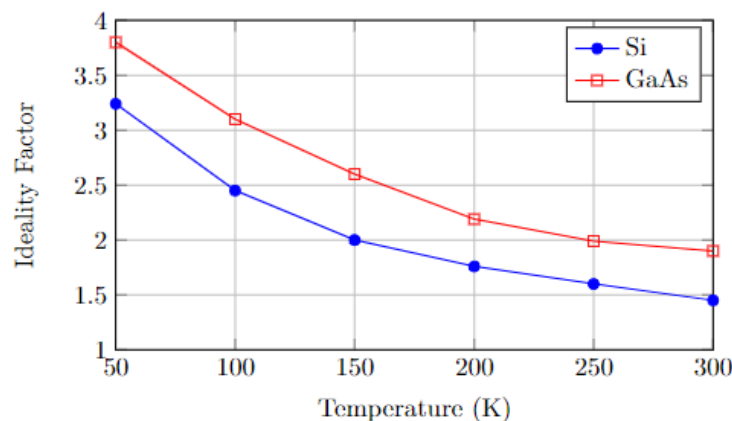


**Figure 5.** Illustrates the temperature dependence of the ideality factor for p-n junctions based on Si and GaAs, ranging from 50 K to 300 K with intervals of 50 K

In Figure 5, utilizing expressions (3) and (4), the following result was derived: the temperature dependence of the ideality factor for p-n junctions based on Si and GaAs, spanning temperatures from 50 K to 300 K with intervals of 50 K. The ideality factor displays a reverse dependence on temperature. This phenomenon arises because, as the temperature decreases, the dominance of the drift-diffusion mechanism diminishes, while the recombination-generation mechanism begins to take precedence. As the temperature decreases, electron diffusion in the Si crystal decreases, as well as in other crystals.

## CONCLUSIONS

In this study, the ideality factor was found to depend on several factors. It was observed that the ideality factor decreases with increasing temperature. Additionally, the ideality factor dependent voltage from 0 to 1 volt for the appropriate connection voltage in silicon. Changes in the ideality factor were also observed when the thickness of the intrinsic layer varied from 10  $\mu\text{m}$  to 100  $\mu\text{m}$ . In all cases where the thickness of the intrinsic i-layer was less than 100  $\mu\text{m}$ , distinct lines were observed at low voltages, while they converged and overlapped at high voltages. Moreover, the influence of the specific concentration of the intrinsic layer on the ideality factor was investigated as it ranged from  $n_i = 10^{11} \text{ cm}^{-3}$  case to  $n_i = 10^{15} \text{ cm}^{-3}$  case. As a result, it was determined that both external and internal factors affect the ideality factor by influencing the current transport mechanism.

## ORCID

Jo'shqin Sh. Abdullayev, <https://orcid.org/0000-0001-6110-6616>; Brokhim B. Sapaev, <https://orcid.org/0000-0003-2365-1554>

## REFERENCES

- [1] S.M. Sze, and K.K. Ng, *Physics of Semiconductor Devices*, third edition, (John Wiley & Sons, Inc., 2007).
- [2] E. Gnani, A. Gnudi, S. Reggiani, and G. Baccarani, *IEEE Trans. Electron Devices*, **58**(9), 2903 (2011). <https://doi.org/10.1109/TED.2011.2159608>
- [3] Z. Arefinia, A. Asgari, *Solar Energy Materials and Solar Cells*, **137**, 146 (2015). <https://doi.org/10.1016/j.solmat.2015.01.032>
- [4] O.V. Pylypova, A.A. Evtukh, P.V. Parfenyuk, I.I. Ivanov, I.M. Korobchuk, O.O. Havryliuk, and O.Yu. Semchuk, *Opto-Electronics Review*, **27**(2), 143 (2019). <https://doi.org/10.1016/j.opelre.2019.05.003>
- [5] R. Ragi, R.V.T. da Nobrega, U.R. Duarte, and M.A. Romero, *IEEE Trans. Nanotechnol.* **15**(4), 627 (2016). <https://doi.org/10.1109/TNANO.2016.2567323>
- [6] R.D. Trevisoli, R.T. Doria, M. de Souza, S. Das, I. Ferain, and M.A. Pavanello, *IEEE Trans. Electron Devices*, **59**(12), 3510 (2012). <https://doi.org/10.1109/TED.2012.2219055>
- [7] N.D. Akhavan, I. Ferain, P. Razavi, R. Yu, and J.-P. Colinge, *Appl. Phys. Lett.* **98**(10), 103510 (2011). <https://doi.org/10.1063/1.3559625>
- [8] A.V. Babichev, H. Zhang, P. Lavenus, F.H. Julien, A.Y. Egorov, Y.T. Lin, and M. Tchernycheva, *Applied Physics Letters*, **103**(20), 201103 (2013). <https://doi.org/10.1063/1.4829756>
- [9] D.H.K. Murthy, T. Xu, W.H. Chen, A.J. Houtepen, T.J. Savenije, L.D.A. Siebbeles, *et al.*, *Nanotechnology*, **22**(31), 315710 (2011). <https://doi.org/10.1088/0957-4484/22/31/315710>

- [10] B. Pal, K.J. Sarkar, and P. Banerji, *Solar Energy Materials and Solar Cells*, **204**, 110217 (2020). <https://doi.org/10.1016/j.solmat.2019.110217>
- [11] J.Sh. Abdullayev, I.B. Sapaev, *Eurasian Physical Technical Journal*, **21**(3), 21–28 (2024). <https://doi.org/10.31489/2024No3/21-28>
- [12] P. Dubey, B. Kaushik, and E. Simoen, *IET Circuits, IET Circuits, Devices & Systems*, (2019). <https://doi.org/10.1049/iet-cds.2018.5169>
- [13] M.-D. Ko, T. Rim, K. Kim, M. Meyyappan, and C.-K. Baek, *Scientific Reports*, **5**(1), 11646 (2015). <https://doi.org/10.1038/srep11646>
- [14] A.M. de Souza, D.R. Celino, R. Ragi, and M.A. Romero, *Microelectronics J.* **119**, 105324 (2021). <https://doi.org/10.1016/j.mejo.2021.105324>
- [15] M.C. Putnam, S.W. Boettcher, M.D. Kelzenberg, D.B. Turner-Evans, J.M. Spurgeon, E.L. Warren, *et al.*, *Energy & Environmental Science*, **3**(8), 1037 (2010). <https://doi.org/10.1039/C0EE00014K>
- [16] Abdullayev, J. S., & Sapaev, I. B. (2024). *East European Journal of Physics*, (3), 344-349. <https://doi.org/10.26565/2312-4334-2024-3-39R>
- [17] Elbersen, R.M. Tiggelaar, A. Milbrat, G. Mul, H. Gardeniers, and J. Huskens, *Advanced Energy Materials*, **5**(6), 1401745 (2014). <https://doi.org/10.1002/aenm.201401745>

### ФАКТОРИ, ЩО ВПЛИВАЮТЬ НА КОЕФІЦІЄНТ ІДЕАЛЬНОСТІ НАПІВПРОВІДНИКОВИХ p-n ТА p-i-n ПЕРЕХІДНИХ СТРУКТУР ПРИ КРІОГЕННИХ ТЕМПЕРАТУРАХ

Джошкін Ш. Абдуллаєв<sup>a</sup>, Іброхім Б. Сапаєв<sup>a,b</sup>

<sup>a</sup>Національний дослідницький університет ТПАМЕ, фізико-хімічний факультет, Ташкент, Узбекистан

<sup>b</sup>Західно-Каспійський університет, Баку, Азербайджан

У цій статті висвітлюється залежність ідеальності фактора як від внутрішніх функціональних параметрів, так і від зовнішніх факторів у напівпровідниках при низьких температурах. Ми дослідили вплив зовнішніх факторів, таких як температура та напруга зовнішнього джерела. За допомогою чисельного моделювання та теоретичного аналізу ми детально вивчили залежності внутрішніх функціональних параметрів напівпровідникових матеріалів, включаючи концентрацію домішок, ширину забороненої зони напівпровідників, тривалість життя носіїв заряду та геометричні розміри в діапазоні від мікрометрів до нанометрів, на ідеальність фактора в структурах p-n і p-i-n переходів. Наш аналіз охоплює криогенні температури від 50 К до 300 К з інтервалом 50 К. Для проведення цього дослідження ми зосередилися на структурах p-n і p-i-n переходів, виготовлених з Si та GaAs. Обрана модель має геометричні розміри  $a=10$  мкм,  $b=8$  мкм і  $c=6$  мкм. Товщина і-шару варіювалася від 10 мкм до 100 мкм з кроком 10 мкм. Збільшення товщини і-шару призводить до відповідного збільшення ідеальності фактора.

**Ключові слова:** p-n перехід; p-i-n перехід; рекомбінація за механізмом Шоклі-Ріда-Холла (SRH); внутрішні функціональні параметри; зовнішні фактори; фактор ідеальності; криогенні температури